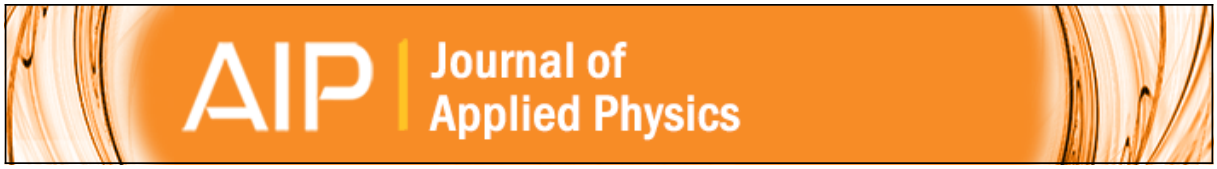

# Relationship between boson heat capacity peaks and evolution of heterogeneous structure in metallic glasses

B. Huang, H. Y. Bai, and W. H. Wang

Citation: Journal of Applied Physics **115**, 153505 (2014); doi: 10.1063/1.4871676
View online: http://dx.doi.org/10.1063/1.4871676
View Table of Contents: http://scitation.aip.org/content/aip/journal/jap/115/15?ver=pdfcov
Published by the AIP Publishing

**Articles you may be interested in**

Pronounced energy absorption capacity of cellular bulk metallic glasses
Appl. Phys. Lett. **104**, 111907 (2014); 10.1063/1.4869229

Characterization of flow units in metallic glass through density variation
J. Appl. Phys. **114**, 123514 (2013); 10.1063/1.4823816

Characterization of flow units in metallic glass through structural relaxations
J. Appl. Phys. **114**, 083512 (2013); 10.1063/1.4819484

Overheating threshold and its effect on time–temperature-transformation diagrams of zirconium based bulk metallic glasses
Appl. Phys. Lett. **84**, 5010 (2004); 10.1063/1.1763219

Thermodynamics of Cu 47 Ti 34 Zr 11 Ni 8 , Zr 52.5 Cu 17.9 Ni 14.6 Al 10 Ti 5 and Zr 57 Cu 15.4 Ni 12.6 Al 10 Nb 5 bulk metallic glass forming alloys
J. Appl. Phys. **87**, 7242 (2000); 10.1063/1.372975

[This article is copyrighted as indicated in the article. Reuse of AIP content is subject to the terms at: http://scitation.aip.org/termsconditions. Downloaded to ] IP: 159.226.35.24 On: Fri, 18 Apr 2014 01:21:59

# Relationship between boson heat capacity peaks and evolution of heterogeneous structure in metallic glasses

B. Huang, H. Y. Bai, and W. H. Wang[a)]
*Institute of Physics, Chinese Academy of Sciences, Beijing 100190, People's Republic of China*

(Received 28 February 2014; accepted 5 April 2014; published online 17 April 2014)

The dependence of boson heat capacity peaks of a typical $Zr_{52.5}Ti_5Cu_{17.9}Ni_{14.6}Al_{10}$ metallic glass on different annealing time and quenching rates is studied. It is found that the boson heat capacity peak moves to higher temperatures and reduces intensity when the metallic glass is isothermally annealed or slowly quenched. We show that the intensity and position change of the boson heat capacity peak are associated with the evolution of heterogeneous structure and inelastic regions in metallic glasses. The results might help in understanding the structural features and evolution as well as their effects on boson peak of metallic glasses. © *2014 AIP Publishing LLC*.
[http://dx.doi.org/10.1063/1.4871676]

## I. INTRODUCTION

Metallic glasses (MGs) show a broad spectrum of elasticity,[1,2] plasticity,[3] toughness,[4] relaxations,[5–7] and other properties even they have the same composition and similar disordered structure frozen from melts.[8–11] These unique characteristics attract intensive researching interest in the last decades. Many theories and models, such as the free-volume theory,[12,13] shear-transformation-zone (STZ) theory,[14,15] and interstitialcy theory,[16,17] have been put forward to explain the fundamental phenomena in MGs. Images of microstructure obtained by scanning electron microscopes (SEM) and transmission electron microscopes (TEM),[3,18] wide distributions of energy dissipation and local indentation modulus detected with atomic force microscopes (AFM),[19,20] mechanical hysteresis in dynamical tests,[6,21] apparent $\beta$ relaxation peaks in the dynamic mechanical spectroscopy (DMA),[6] and other experiments[22] have demonstrated the nano-scale heterogeneous structure of MGs. The MG then can be considered as a composite of nano-scale loose and elastic dense atomic packing regions, and the fraction of the liquid like regions or flow units correlates with the mechanical properties and characteristics in a MG.[18–25] The structural metallic glassy model supports some of the proposed theories and can explain abundant mechanical and relaxation behaviors in MGs.[1–7,10,11] However, the evolution of the heterogeneous microstructure of MGs at different glassy states as well as its relationship with the boson peak has scarcely been investigated by the low temperature heat capacity which can reflect vibrational behaviors of the microstructure of MGs.[26–33]

Like other glasses, MGs display broad bumps in $C'_p/T^3$ plot appear at about 10 K, where the $C'_p$ is the heat capacity contributed by the disordered atoms.[27–33] The low temperature heat capacity bumps for series of glasses like $Pd_{40}Cu_{40}P_{20}$, $B_2O_3$, $SiO_2$, and $GeO_2$, which are the excess of vibrational density of states (VDOSs) over the Debye contribution,[27,29,34] are called the boson peak and have been attributed to the dispersion of acoustic phonons and/or excitation of optical phonons.[35] The low-temperature anomaly, which was found to be universal exhibited by almost all kinds of glasses, is still a unsolved and debated issue of condensed matter physics. A number of theoretical models, such as the soft potential model,[36,37] the interstitialcy theory,[38,39] the mode-coupling approach,[40] and the resonant modes involving loosely bound structural fragments,[41] atom clusters[42] or strings of atoms,[43] and others[44,45] have been proposed to explain the structural origin and mechanism of boson peaks. Simulations reveal that spatially fluctuating interatomic force constants[46] and microscopic shear stresses[47] can also produce boson peaks. With increasing pressure, the transformation of the boson peak of $NaFeSi_2O_6$ glass towards the transverse acoustic singularity of the crystalline counterpart suggests that piling up of transverse acoustic singularity could lead to the boson peak.[48] Many studies have been performed on the dependence of the boson peak from an external parameter or from the previous thermal history and the results are sometimes controverted.[49–53] The majority of these studies deal with molecular, network, and polymeric glasses and very little is known on the boson peak and its link with the heterogeneous structure in MGs.[27,28,31–33]

In this paper, we selected a typical $Zr_{52.5}Ti_5Cu_{17.9}Ni_{14.6}Al_{10}$ MG (Vit105) as a model system to study the low temperature heat capacity anomalies in MGs as a function of the previous thermal path and the quenching rate used to produce the glass. The excellent glass forming ability and high thermal stability of Vit105 guarantee the fully amorphous structure when it was isothermal annealed for different times and quenched with different cooling rates.[54,55] The mechanical behaviors, elastic constants, Poisson ratios ($\nu$), relaxations, and densities ($\rho$) of the as cast and isothermally annealed Vit105 have been previously systematically studied.[10,11] The boson heat capacity peak, i.e., the bump in $C'_p/T^3$ plot of the MG, is found to be sensitive to both the annealing time and quenching rate. We deduce the distribution of energies of the excess vibrational modes and correlate the boson heat capacity peaks with the evolution of the structural heterogeneity and inelastic regions of the MG at different glassy states.

a)Author to whom correspondence should be addressed. Electronic mail: whw@iphy.ac.cn.

 © 2014 AIP Publishing LLC

[This article is copyrighted as indicated in the article. Reuse of AIP content is subject to the terms at: http://scitation.aip.org/termsconditions. Downloaded to ] IP: 159.226.35.24 On: Fri, 18 Apr 2014 01:21:59

The results have implications for understanding the structural evolution features at different glassy states and the structural origin of boson peaks of MGs.

## II. EXPERIMENTAL DETAILS

Cylindrical rods of Vit105 in diameter of 2 mm and 5 mm were fabricated with the copper mold casting method. The critical cooling rate ($R_c$) for the MG can be estimated with $R_c = A/\phi^2$, where $A$ equals to 10 K·cm$^2$·s$^{-1}$ and the diameter of the rod $\phi$ is measured in cm.[56] The values of $R_c$ of Vit105 rods with $\phi = 2$ mm and 5 mm are about 250 K/s and 40 K/s, respectively. A square-shaped plate with a size of $3\times3\times1$ mm$^3$ was cut near the center of the 5 mm rod and annealed for 15 min, 30 min, 1 h, 8 h, and 32 h at 600 K (71 K below the glass transition temperature $T_g$). The isothermal annealing below the $T_g$ leads to lower potential energies in the energy landscape and different glassy configurations for the MG. The amorphous structure of all the as cast and annealed Vit105 specimens was confirmed by X-ray diffraction (XRD) and differential scanning calorimetry (DSC). The DSC experiment was performed with a power compensated Perkin-Elemer DSC 8000 with a heating rate of 0.33 K/s under a constant flow of high purity argon gas. We also prepared a Vit105 sample through cooling the supercooled liquid from 713 K to room temperature without the copper mold. The XRD demonstrated that the alloy is almost polycrystalline phases because its cooling rate was less than the critical one for the full amorphous formation of the alloy. The measurements of heat capacity $C_p$ (error $< 2\%$) for all the samples were carried out with a physical property measurement system (PPMS 6000) of Quantum Design from 2.0 K to 101 K. For metallic glasses, the $(C_p - C_V)/C_p$ are less than 0.1% in the measuring temperature range, we then uses $C_p$ instead of $C_V$ in the work for convenience.

## III. RESULTS AND DISCUSSIONS

The heat capacities $C_p$ between 2.0 K and 100 K for as cast 2 mm and 5 mm Vit105, and 32 h annealed Vit105 are shown in the inset of Fig. 1(a). The heat capacity difference around 10 K for these samples where boson peaks influence is not obvious in their total specific heat curves. $C_p/T$ has linear relations with $T^2$ below 8 K for the MG as shown in Fig. 1(a). We fit the $C_p$ data in low temperature range with the formula $C_p/T = \gamma + \beta T^2$, where $\gamma$ represents the Sommerfeld coefficient. The fitting $\gamma$ and $\beta$ for the as cast 2 mm, 5 mm, and the annealed Vit105 are listed in Table I. We notice that $\gamma$ is smaller for the as cast MG formed with a smaller $R_c$ and the MG annealed for longer time. In metals, $\gamma$ can be expressed as $\gamma = (\pi^2/3)k_B^2 N(E_F)$, where $N(E_F)$ represents the electronic density of states at the Fermi level.[60] When $E_F$ is far from the pseudogap in the structure of energy bands, and the $N(E_F)$ decreases with the increase of density of free electrons as predicted by the nearly free electron model.[57] So, supposing the total number of free electrons keeps constant, the decease of $\gamma$ corresponds to the increase of density $\rho$ and the lowering of the potential energy for 5 mm Vit105.

Specific heat $C'_p$ contributed by the vibrations of disordered structure is obtained through subtracting electronic heat capacity $\gamma T$ from the total $C_p$. Figure 1(b) shows $(C_p - \gamma T)/T^3$ versus $T$ in a semilogarithmic scale for the as cast 2 and 5 mm Vit105, 15 min, 1 h, 8 h, and 32 h annealed Vit105. Broad boson heat capacity humps appear in the $(C_p - \gamma T)/T^3$ curves for all the samples around 10 K, which is beyond the explanation of the Debye elastic model[57] and the two-level tunneling effect[58] existing below 1 K. The maxima of the humps $[(C_p - \gamma T)/T^3]_{max}$ and the corresponding temperature $T_{max}$ are listed in Table I. The boson heat capacity peaks become less pronounced and move to higher temperatures for as cast MG formed with a smaller $R_c$ and MGs annealed for longer time. Below 4 K perhaps, due to the contribution of the two level systems, the $C_p$ deviates from the fitting results based on our model. We also measured the $C_p$ of 2 mm Vit105 annealed for different time at 600 K (not shown here), and the changing trend of boson heat capacity peaks with aging is similar to that for 5 mm annealed Vit105. This indicates that the boson heat capacity peaks are influenced by the microstructure of the glasses at different states. We also measured the polycrystalline formed with a very small $R_c$ (with little fraction of glassy phase) and find that a

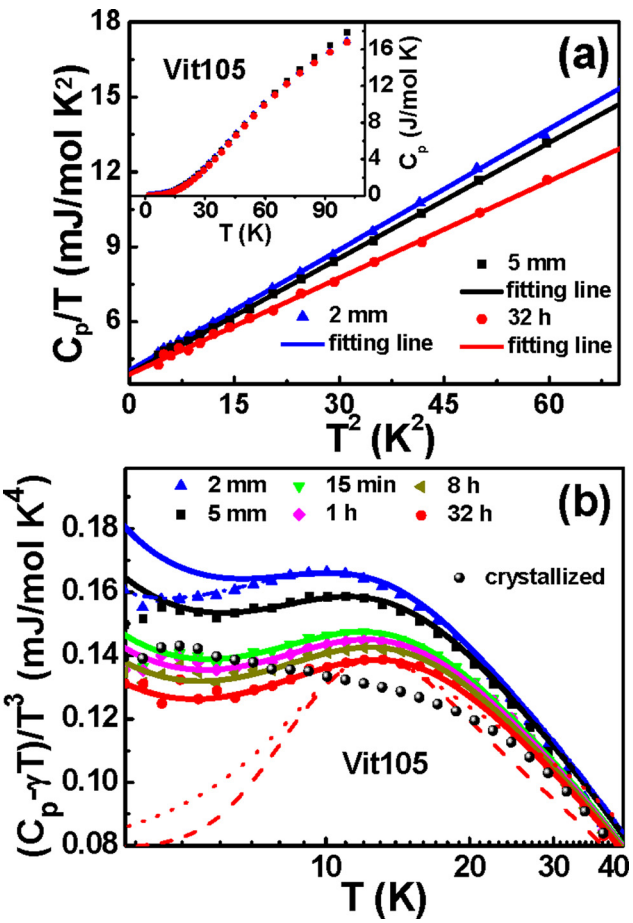


FIG. 1. (a) $C_p/T$ versus $T^2$ below 8 K for as cast 2 mm and 5 mm, 32 h annealed Vit105. The lines are the fitting results. The inset shows the $T$ dependent $C_p$ between 2.0 K and 101 K for the MGs. (b) $(C_p - \gamma T)/T^3$ versus $T$ in a semilogarithmic scale for the as cast, annealed, and slowly quenched Vit105 (containing mostly crystalline phases). The red dashed line is the fitting line with Eq. (2), the solid lines are the fitting lines with Eq. (5), and the red dotted line is the fitting line with the model considering the interaction of low frequency excess modes. The blue dashed-dotted line is the fitting result.

[This article is copyrighted as indicated in the article. Reuse of AIP content is subject to the terms at: http://scitation.aip.org/termsconditions. Downloaded to ] IP: 159.226.35.24 On: Fri, 18 Apr 2014 01:21:59

TABLE I. The fitting $\gamma$ and $\beta$ with the equation $C_p/T = \gamma + \beta T^2$ below 8 K, the maxima of boson heat capacity peaks $[(C_p - \gamma T)/T^3]_{max}$, and the corresponding temperatures $T_{max}$, the fictive temperatures $T_f$, and Poisson ratios $\nu$ for the as cast and annealed Vit105.

| Vit105 | $\gamma$ (mJ/mol K$^2$) | $\beta$ (mJ/mol K$^4$) | $T_{max}$ (K) | $[(C_p - \gamma T)/T^3]_{max}$ (mJ/mol K$^4$) | $T_f$ (K) | $\nu$ |
|---|---|---|---|---|---|---|
| 2 mm | 4.053 | 0.1604 | 10.053 | 0.1664 | 717.3[a] | … |
| 5 mm | 3.923 | 0.1542 | 11.011 | 0.1586 | 700.7[b] | 0.3722[c] |
| 15 min | 3.913 | 0.1404 | 12.020 | 0.1473 | 687.6[b] | … |
| 1 h | 3.912 | 0.1375 | 12.026 | 0.1446 | 681.7[b] | … |
| 8 h | 3.896 | 0.1347 | 12.032 | 0.1425 | 670.9[b] | 0.3674[c] |
| 32 h | 3.888 | 0.1291 | 13.167 | 0.1387 | 659.4[b] | 0.3664[c] |

[a]This work.
[b]Reference 61.
[c]Reference 59.

broad peak appears at 3.8 K, and the peak intensity is larger than the $(C_p - \gamma T)/T^3$ value for 15 min, 1 h, 8 h, and 32 h annealed 5 mm Vit105 as shown in Fig. 1(b). The complex change of the glassy structure during crystallization obviously affects the boson heat capacity peak.

The thermal history dependence of the glassy state can be accounted for the evolution of the fictive temperature $T_f$.[59–61] We determine the $T_f$ of as cast 2 mm Vit105 based on the release enthalpy measured with DSC using the method proposed by Hodge.[60] The $T_f$ of 5 mm Vit105 is obtained from Ref. 62, which was obtained with the same method. The values of $T_f$ for the Vit105 in different glassy states are listed in Table I. With increasing annealing time or decreasing quenching rates, the $T_f$ decreases corresponding to the increase of density $\rho$ (Ref. 62) and implying the low energy configuration states in the energy landscape. Figure 2 shows that the intensity of the boson heat capacity peak decreases with the decrease of $T_f$ of Vit105. As the decrease of $T_f$ is related to the microstructure, the change of boson heat capacity peaks should closely correlate with the evolution of the loosely packed regions in the glasses of Vit105. With increasing annealing time and deceasing $[(C_p - \gamma T)/T^3]_{max}$, the shear modulus $G$ also increases for 5 mm Vit105 implying the similar evolution of the microstructure in the MGs which is consistent with the experimental result of bulk $Pd_{41.25}Cu_{41.25}P_{17.5}$ metallic glass.[26]

The MGs with heterogeneous structure can be regarded as a composite of soft regions exhibiting a lower packing density and the elastic matrix. The soft regions have a relatively lower local elastic modulus, smaller hardness, and a higher energy dissipation rate than the matrix as shown in Figs. 3(a) and 3(b). Intensive experimental results demonstrate that the heterogeneous structure with higher concentrations of flow units, which can be signified by relatively large Poisson ratios $\nu$, is responsible for the better plasticity of MGs.[3,63] Figure 2 also shows that the $[(C_p - \gamma T)/T^3]_{max}$ of Vit105 increases with the increase of $\nu$, and this indicates that the higher intensity of the boson heat capacity peak is suggestive of more inhomogeneous structure and better plasticity of a MG. Next, we will further analyze the relationship between boson heat capacity peaks and the heterogeneous structure in MGs.

Independent localized harmonic vibrations of loosely or weakly bound atoms or atomic clusters can be described by Einstein-type modes which have been found in Ni-,[31] Ca-,[32] and CuZr-based[27] bulk MGs. For an independent harmonic vibration, the energy $E$ of the vibrational mode can be expressed as[57]

$$E = k_B\theta_E = -h\sqrt{C/M}, \quad (1)$$

where $C$ is the force constant between the vibrational atoms/clusters and the densely packed matrix, and $M$ represents the mass of the atom/cluster. The $C$ will increase if the distance between the atom/cluster and the matrix decreases. So $E$ can reflect the local elastic moduli and densities of samples and they should be smaller if more loosely bonded atoms/clusters

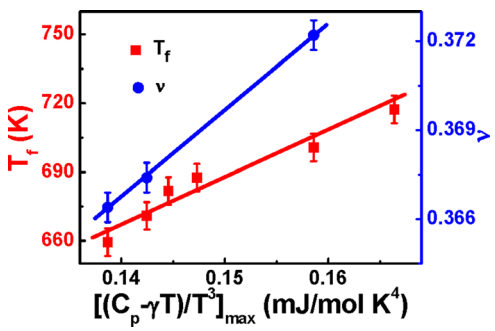


FIG. 2. The fictive temperature $T_f$ and Poisson ratio $\nu$ versus the boson heat capacity peak value $[(C_p - \gamma T)/T^3]_{max}$ for Vit105 at different glassy states.

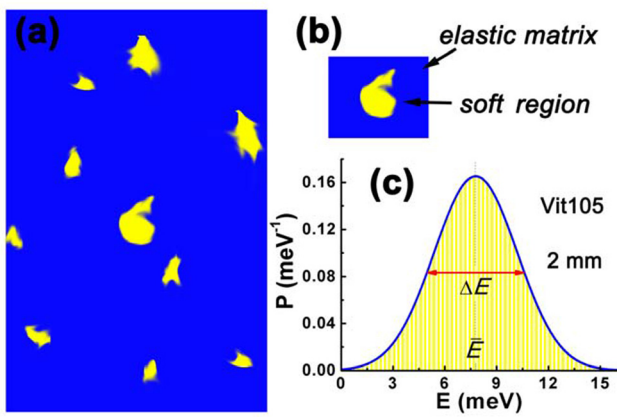


FIG. 3. (a) and (b) Schematic illustration of the structural heterogeneity. The soft regions and elastic matrix are marked by yellow and blue zones, respectively. (c) The distribution of energies of excess vibrational modes for Vit105 (2 mm) calculated with Eq. (7) (the blue line).

[This article is copyrighted as indicated in the article. Reuse of AIP content is subject to the terms at: http://scitation.aip.org/termsconditions. Downloaded to ] IP: 159.226.35.24 On: Fri, 18 Apr 2014 01:21:59

with lower vibrational frequencies exist in the localized region. Considering the existence of weak atomic bonding in the nanoscale soft regions, we try to use excess localized vibrational modes to describe the vibrations of the loosely bonded atoms/clusters in the soft regions or flow units and the boson heat capacity peaks of Vit105 at different glassy states.

We introduce an additional Einstein mode to interpret the boson heat capacity peak of Vit105 annealed for 32 h, and the total $C_p$ is expressed as

$$C_p = \gamma T + n_D C_D + n_E C_E, \tag{2}$$

where $n_D$ and $n_E$ represent the Debye and Einstein oscillator strength per mole, respectively. The Debye term $C_D$ can be expressed as

$$C_D = 9R\left(\frac{T}{\theta_D}\right)^3 \int_0^{\theta_D/T} \frac{\xi^4 e^\xi}{(e^\xi - 1)^2} d\xi, \tag{3}$$

where $R$ and $\theta_D$ are the universal gas constant and Debye temperature, respectively. $\theta_D$ for Vit105 listed in Table II are obtained with the fitting or with acoustic velocities measured with a pulse echo overlap method (the frequency of the ultrasonic waves is 10 MHz). The Einstein term $C_E$ can be expressed as

$$C_E = 3R\left(\frac{\theta_E}{T}\right)^2 \frac{e^{\theta_E/T}}{(e^{\theta_E/T} - 1)^2}, \tag{4}$$

where $\theta_E$ is the Einstein temperature. The best fitting line for the boson heat capacity peak with Eq. (2) is shown in Fig. 1(b) (the red dashed curve). The $n_D$, $n_E$, and $\theta_E$ are obtained as 0.9724, 0.0276, and 62.8 K, respectively. One can see that the $(C_p - \gamma T)/T^3$ hump is much broader than the fitting curve, and this indicates that there exist an energy distribution of the Einstein modes for the MG.

It has been reported that the local elastic properties over the surface of PdCuSi MG[20] and the activation energies of deformation units[22] approximately have Gaussian distributions. We therefore suggest that the energies of excess Einstein modes also obey Gaussian distributions for Vit105. We rewrite Eq. (2) as

$$C_p = \gamma T + n_D C_D + \int_0^\infty C_E \bullet [n_E \bullet \chi(\theta_E, \bar{\theta}_E, \sigma_E)] d\theta_E. \tag{5}$$

The Gaussian function $\chi(\theta_E, \bar{\theta}, \sigma_E)$ can be expressed as

TABLE II. The Debye temperatures $\theta_D$, the mean energies of excess vibrational modes $\bar{E}$, and the number of vibrational modes with energies below 7.793 meV $N$.

| Vit105 | $\theta_D$ (K) | $\bar{E}$ (meV) | $N$ |
|---|---|---|---|
| 2mm | 278.0[a] | 7.793 | 0.0340 |
| 5mm | 278.3[b] | 7.948 | 0.0322 |
| 15 min | 284.0[a] | 8.103 | 0.0305 |
| 1 h | 285.0[b] | 8.146 | 0.0300 |
| 8 h | 285.8[b] | 8.198 | 0.0294 |
| 32 h | 287.5[b] | 8.276 | 0.0286 |

[a]The fitting results.
[b]Reference 59.

$$\chi(\theta_E, \bar{\theta}_E, \sigma_E) = \frac{1}{\sigma_E \sqrt{2\pi}} e^{-\frac{(\theta_E - \bar{\theta}_E)^2}{2\sigma_E^2}}, \tag{6}$$

where $\bar{\theta}_E$ and $\sigma_E$ are the mean and standard deviation of the distribution, respectively. The best fitting result of the $(C_p - \gamma T)/T^3$ hump for 32 h annealed Vit105 with Eq. (4) is shown in Fig. 1(b) (the red solid curve). The fitting curve well matches the experimental data in a large temperature range of about 40 K indicating the appropriateness of the Gaussian distribution of energies of excess Einstein modes. The fitting curves of boson heat capacity peaks with Eq. (4) for all the Vit105 samples in different glassy states are also shown in Fig. 1(b) (the solid curves). It can be seen that all the boson heat capacity peaks are well fitted. The fitting $n_D$, $n_E$, and $\sigma_E$ are about 0.932, 0.068, and 26.0 K for the MGs at different glassy states. $\bar{\theta}_E$ is between 90 K and 100 K and increases with the decrease of $[(C_p - \gamma T)/T^3]_{max}$.

The measurement time windows for the data around the boson heat capacity peak are about 10 s. The vibrations with frequencies smaller than 0.1 Hz or with energies smaller than $10^{-16}$ meV cannot be reflected from the boson heat capacity peaks and will hardly influence the above fitting results. The contribution of one vibrational mode with a frequency larger than $10^{13}$ Hz or with $\theta_E$ larger than 500 K to the heat capacity around 10 K can be estimated to be less than $10^{-10}$ J/mol K with Eq. (4). So our fitting results cannot accurately describe the vibrations with high frequencies much larger than those of boson peaks (in the order of $10^{12}$ Hz). The energy $E$ distributions of excess vibrational modes with frequencies from 0.1 Hz to $10^{13}$ Hz for the studied Vit105 can be expressed as

$$P = \chi(\theta_E, \bar{\theta}_E, \sigma_E)/k_B. \tag{7}$$

With Eq. (7), the $E$ distribution, the corresponding mean energy value $\bar{E}$ ($\bar{E} = k_B \bar{\theta}_E$), and full width at half maximum $\Delta E$ for as cast Vit105 ($\phi = 2$ mm) are shown in Fig. 3(c) (the blue curve). The Gaussian distribution of $E$ suggests that the soft region could not be regarded as one type of localized atoms or clusters or a single phase and no well-defined physical boundary between the soft region and the elastic matrix exist in MGs. The large value 0.730 of $\Delta E/\bar{E}$ reflecting the fluctuations of vibrational energies or local moduli confirms the high degree of microstructural heterogeneity. We note that the boson heat capacity peak can be fit more completely including the low temperature side of the peak through adding another distribution to the one Gaussian distribution for 2 mm as cast Vit105 [see the blue dashed-dotted curve shown in Fig. 1(b)]. The modified distribution of $E$ exhibits no significant difference.

The aging effects on boson heat capacity peaks of many other glasses have been studied.[44,45,64–69] However, due to the various and sometimes contradictive experimental results and the complex structure of glasses, the origins of the phenomena remain controversial. During the aging process, the Debye temperature changes little for one kind of vitreous silica, and the phonons dispersion is not contributed significantly to the excess heat capacity;[67] while for dry $B_2O_3$ glasses, the boson heat capacity peak changes which is

[This article is copyrighted as indicated in the article. Reuse of AIP content is subject to the terms at: http://scitation.aip.org/termsconditions. Downloaded to ] IP: 159.226.35.24 On: Fri, 18 Apr 2014 01:21:59

mainly induced by the change of the Debye temperature.[68] Recent experiments show that the rejuvenation of hyperageing amber only increases the heat capacity contributed by elastic parts and the excess heat capacity is hardly influenced.[69] Our experimental results of Vit105 show that the heat capacities are contributed by both of the elastic parts and the loose atoms/clusters in the soft regions decrease when it is annealed. The decrease of excess heat capacity is associated with the change of the distribution of the excess low frequency vibrational modes and the soft regions as will be discussed below. We analyze the VDOSs of Vit105 to explore the structural change at different glassy states. The total VDOS divided by $3N$ ($N$ is the Avogadro's number) for the studied MGs can be expressed as[57]

$$g(E) = n_D \bullet 3E^2/(k_B\theta_D)^3 + n_E \bullet \chi(\theta_E, \bar{\theta}_E, \sigma_E)/k_B. \quad (8)$$

With the fitting results in Fig. 1(b), the obtained $g(E)/E^2$ for all the studied MG samples are depicted in the inset of Fig. 4. The blue, black, green, magenta, dark yellow, and red dashed line represent the Debye contributions to $g(E)/E^2$ for the as cast 2 mm and 5 mm, 15 min, 1 h, 8 h, and 32 h annealed Vit105 samples, respectively. The $g(E)/E^2$ shows broad peaks around 7 meV, and the peak moves to higher energies and has lower intensities for the samples formed with a smaller $R_c$ or annealed for longer time. The intensity of the boson peak decreases with the increase of $\rho$ and the decrease of $T_f$ similar to the cases in nonmetallic glasses such as polymers,[50,70] silica,[71] $Na_2FeSi_3O_8$,[49] and $NaFeSi_2O_6$.[48]

The low frequency vibrational states can also be studied by Raman scattering, inelastic neutron scattering, infrared absorption, heat capacity, and so on. With a proper frequency-dependent coupling factor, the VDOS of a glass obtained could be the same.[72] We notice that the shapes of the obtained total VDOSs of Vit105 are different from those of some other non-metallic glasses like vitreous silica, $a$-$B_2O_3$, and ethanol deduced from neutron scattering or Raman scattering.[73] With introducing the interaction of low frequency vibrations, the spectrum of vibrational modes can well explain the VDOSs of the glasses.[73] They derive the form of the VDOSs of low frequency vibrations (excluding the Debey part at low frequencies) as

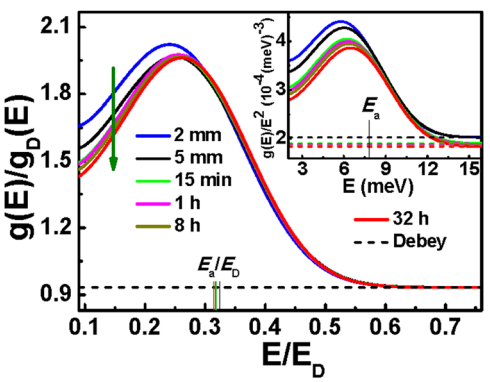


FIG. 4. The total VDOS in Debye units and the Debye contribution for Vit105 at different glassy states. The inset shows $E$ dependent $g(E)/E^2$ and the Debye contribution for Vit105 at different glassy states.

$$\frac{g(\omega)}{\omega^2} = \frac{3C}{\pi\omega^*}\left(\frac{\omega^*}{\omega}\right)^4 [z_1^2(\omega) + z_2^2(\omega)]^{-1} \times \left[\frac{1}{2z_1(\omega)}\ln\frac{z_1(\omega)+1}{z_1(\omega)-1} + \frac{1}{z_2(\omega)}\tan^{-1}\frac{1}{z_2(\omega)}\right], \quad (9)$$

where $\omega$ is the vibrational frequency, $C$ is a constant and $z_{1,2}(\omega) = \frac{1}{2}\sqrt{\sqrt{9+8(\omega^*/\omega)^6} \pm 3}$, with $\omega^*$ characterizing the position of the boson peak. We also attempt to fit the $(C_p\text{-}\gamma T)/T^3$ hump of 32 h annealed Vit105 with the excess VDOS described by Eq. (9) and the result is shown in Fig. 1(b) (the red dotted line). The worse fitting implies that Vit105 has a different type of structure compared with that of the glasses like a-$SiO_2$ and the interaction of excess low frequency modes could be very weak in for Vit105 MG.

In order to evaluate the role of inelastic medium, the $E/E_D$ dependent $g(E)/g_D(E)$ for as cast and annealed Vit105 rescaled in Debye units are as shown in Fig. 4. $E_D$ and $g_D(E)$ are the Debey energy and Debye contribution to the total VDOS, respectively. The curves of 5 mm as cast and annealed Vit105 samples nearly rescale on a master curve in the peak region and in the region with higher energies. A similar scaling has also been observed in the case of network, molecular, and polymeric glasses under temperature and pressure changes, suggesting a more general scenario.[49,51,52] The soft regions of 5 mm Vit105 containing the loosely bonded atoms/clusters with low energy vibrational modes and transform inelastically through structural relaxations or atomic diffusion, since the structural change cannot be described as Debye elastic continuum. The 2 mm Vit105 quenched with a higher cooling rate has a more pronounced $g(E)/g_D(E)$ peak as much more liquid-like soft regions or inhomogeneous with vibrational energies in the peak region are frozen in the glass. The narrowing of $g(E)/g_D(E)$ peaks for the as cast 2 mm and 5 mm, 15 min, 1 h, 8 h, and 32 h annealed Vit105 in Fig. 4 suggests that the Vit105 annealed for longer time or quenched at a slower rate has more homogeneous structure due to the inelastic transformation of the soft regions. We will analyze the VDOS of excess modes describing the soft regions or potential flow units in the quenching and annealing process in the following.

The VDOS of excess modes describing the vibrations of the atoms/clusters in soft regions in Fig. 3(a) can be expressed as

$$n = n_E \bullet \chi(\theta_E, \bar{\theta}_E, \sigma_E)/k_B. \quad (10)$$

Figure 5(a) shows the VDOS of excess modes for the studied Vit105. One can see that the Vit105 annealed for longer time or quenched at a slower rate have less low energy vibrational modes and more high energy vibrational modes. The mean energies $\bar{E}$ [corresponding to the peak as indicated in Fig. 5(a) and listed in Table II] increase with the decrease of $[(C_p - \gamma T)/T^3]_{max}$ as shown in Fig. 5(b). This means that the soft regions in the longer time annealed MG or more slowly quenched as cast MG have higher vibrational energies. The decrease of $[(C_p - \gamma T)/T^3]_{max}$ corresponds to higher activation energy or more stable structure of the loosely packed

[This article is copyrighted as indicated in the article. Reuse of AIP content is subject to the terms at: http://scitation.aip.org/termsconditions. Downloaded to ] IP: 159.226.35.24 On: Fri, 18 Apr 2014 01:21:59

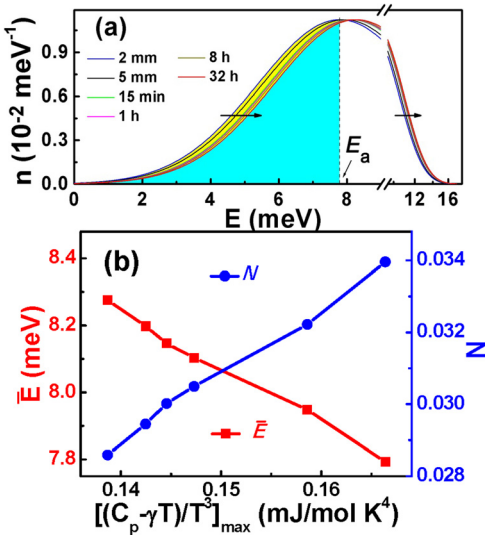


FIG. 5. (a) The VDOS of excess modes for Vit105 at different glassy states. (b) The mean energy of excess modes $\bar{E}$, the number $N$ of excess modes with energies smaller than $E_a$ versus $[(C_p-\gamma T)/T^3]_{max}$ for Vit105 at different glassy states.

soft regions induced by structural evolution. The change of the distribution of the excess low frequency vibrational modes induced by the structural change decreases the excess heat capacity.

The peak energy of 2 mm Vit105, $E_a$ (7.793 meV), is marked in Fig. 5(a). The $E_a$, $E_a/E_D$ for other as cast or annealed Vit105 are also marked in Fig. 4. It can be seen that the obvious invalidity of the scaling in Debye units occurs at energies lower than $E_a$. As indicated by the olive arrow in Fig. 4, the scaled $g(E)/g_D(E)$ in the low temperature range decreases for Vit105 quenched at a slower cooling rate or annealed for longer time. This indicates that the Vit105 obtained with a lower cooling rate or annealed for longer time has fewer excess modes with low energies ($E < E_a$). The number of excess mode $N$ with energies lower than the peak energy $E_a$ can be represented as the area under the excess VDOS curve below $E_a$ as shown in Fig. 5(a). The calculated $N$ for all the samples are listed in Table II. Fig. 5(b) exhibits that the $N$ decreases with the decrease of $[(C_p-\gamma T)/T^3]_{max}$ suggesting the soft regions or potential flow units with low activation energies are annihilated and are relaxed into a more stable state during annealing. The area marked by yellow in Fig. 5(a) represents the reduction of the excess modes for 32 h annealed Vit105 compared with as cast 2 mm Vit105. The decrease of $N$ corresponding to the structural evolution containing the loosely bonded atoms/clusters with low energy vibrational modes in the annealing and quenching process is also the origin of the evolution of the heterogeneity for long time annealed or slowly quenched Vit105.

## IV. CONCLUSIONS

The boson heat capacity peak of Vit105 is sensitive to glassy configurations, and it moves to higher temperatures and has smaller intensities for the MG formed with a smaller cooling rate or annealed for longer time, in agreement with the results observed in nonmetallic glasses. We show that the boson heat capacity peak in MGs is closely correlated with the inhomogeneous structure and loosely packed regions which have Gaussianly distributed vibrational energies of excess modes. The energies of excess vibrational modes as well as the number of loosely packed atoms influence the features of the boson peak in the MG, which can be tuned by annealing or quenching rates. The results could have significance in understanding the effects of the cooling rate, aging on the structure of MGs and the structural origin of boson peaks of MGs.

## ACKNOWLEDGMENTS

The authors are grateful for the experimental assistance and helpful discussions of B. Ruta, D. Q. Zhao, D. W. Ding, S. K. Su, P. Wen, and M. X. Pan. The financial support of the NSF of China (Grant No. 51271195) and MOST 973 of China (No. 2010CB731603) is appreciated.

[1]L. Tian, Y. Q. Cheng, Z. W. Shan, J. Li, C. C. Wang, X. D. Han, J. Sun, and E. Ma, Nat. Commun. **3**, 609 (2012).
[2]J. Yi, X. X. Xia, D. Q. Zhao, M. X. Pan, H. Y. Bai, and W. H. Wang, Adv. Eng. Mater. **12**, 1117 (2010).
[3]Y. H. Liu, G. Wang, R. J. Wang, D. Q. Zhao, M. X. Pan, and W. H. Wang, Science **315**, 1385 (2007).
[4]M. D. Demetriou, M. E. Launey, G. Garrett, J. P. Schramm, D. C. Hofmann, W. L. Johnson, and R. O. Ritchie, Nature Mater. **10**, 123 (2011).
[5]H. B. Yu, W. H. Wang, H. Y. Bai, and M. W. Chen, Phys. Rev. B **81**, 220201 (2010).
[6]Z. Wang, P. Wen, L. S. Huo, H. Y. Bai, and W. H. Wang, Appl. Phys. Lett. **101**, 121906 (2012).
[7]H. B. Yu, Y. S. Luo, and K. Samwer, Adv. Mater. **25**, 5904 (2013).
[8]H. S. Chen, Rep. Prog. Phys. **43**, 353 (1980).
[9]W. L. Johnson, JOM **54**, 40 (2002).
[10]W. H. Wang, Prog. Mater. Sci. **52**, 540 (2007).
[11]W. H. Wang, Prog. Mater. Sci. **57**, 487 (2012).
[12]D. Turnbull and M. H. Cohen, J. Chem. Phys. **34**, 120 (1961).
[13]P. Ramachandrarao, B. Cantor, and R. W. Cahn, J. Mater. Sci. **12**, 2488 (1977).
[14]M. J. Demkowicz and A. S. Argon, Phys. Rev. Lett. **93**, 025505 (2004).
[15]J. S. Langer, Phys. Rev. E **77**, 021502 (2008).
[16]A. Granato and V. Khonik, Phys. Rev. Lett. **93**, 155502 (2004).
[17]K. Nordlund, Y. Ashkenazy, R. S. Averback, and A. V. Granato, Europhys. Lett. **71**, 625 (2005).
[18]H. B. Yu, X. Shen, Z. Wang, L. Gu, W. H. Wang, and H. Y. Bai, Phys. Rev. Lett. **108**, 015504 (2012).
[19]Y. H. Liu, D. Wang, K. Nakajima, W. Zhang, A. Hirata, T. Nishi, A. Inoue, and M. W. Chen, Phys. Rev. Lett. **106**, 125504 (2011).
[20]H. Wagner, D. Bedorf, S. Küchemann, M. Schwabe, B. Zhang, W. Arnold, and K. Samwer, Nature Mater. **10**, 439 (2011).
[21]J. C. Ye, J. Lu, C. T. Liu, Q. Wang, and Y. Yang, Nature Mater. **9**, 619 (2010).
[22]W. Jiao, P. Wen, H. L. Peng, H. Y. Bai, B. A. Sun, and W. H. Wang, Appl. Phys. Lett. **102**, 101903 (2013).
[23]T. Ichitsubo, E. Matsubara, T. Yamamoto, H. S. Chen, N. Nishiyama, J. Saida, and K. Anazawa, Phys. Rev. Lett. **95**, 245501 (2005).
[24]L. S. Huo, J. F. Zeng, W. H. Wang, C. T. Liu, and Y. Yang, Acta Mater. **61**, 4329 (2013).
[25]B. Huang, H. Y. Bai, P. Wen, D. W. Ding, D. Q. Zhao, M. X. Pan, and W. H. Wang, J Appl. Phys. **114**, 113508 (2013).
[26]A. S. Makarov, V. A. Khonik, Y. P. Mitrofanov, A. V. Granato, D. M. Joncich, and S. V. Khonik, Appl. Phys. Lett. **102**, 091908 (2013).
[27]Y. Li, H. Y. Bai, W. H. Wang, and K. Samwer, Phys. Rev. B **74**, 052201 (2006).
[28]A. N. Vasiliev, T. N. Voloshok, A. V. Granato, D. M. Joncich, Yu. P. Mitrofanov, and V. A. Khonik, Phys. Rev. B **80**, 172102 (2009).

[This article is copyrighted as indicated in the article. Reuse of AIP content is subject to the terms at: http://scitation.aip.org/termsconditions. Downloaded to ] IP: 159.226.35.24 On: Fri, 18 Apr 2014 01:21:59

[29]R. C. Zeller and R. O. Pohl, Phys. Rev. B **4**, 2029 (1971).
[30]M. B. Tang, H. Y. Bai, and W. H. Wang, Phys. Rev. B **72**, 012202 (2005).
[31]Z. Zhou, C. Uher, D. Xu, W. L. Johnson, W. Gannon, and M. C. Aronson, Appl. Phys. Lett. **89**, 031924 (2006).
[32]V. Keppens, Z. Zhang, O. N. Senkov, and D. B. Miracle, Philos. Mag. **87**, 503 (2007).
[33]Y. Li, P. Yu, and H. Y. Bai, J Appl. Phys. **104**, 013520 (2008).
[34]U. Buchenau, Yu. M. Galperin, V. L. Gurevich, and H. R. Schober, Phys. Rev. B **43**, 5039 (1991).
[35]D. J. Safarik, R. B. Schwarz, and M. F. Hundley, Phys. Rev. Lett. **96**, 195902(2006).
[36]D. A. Parshin, Phys. Rev. B **49**, 9400 (1994).
[37]D. A. Parshin, H. R. Schober, and V. L. Gurevich, Phys. Rev. B **76**, 064206 (2007).
[38]A. V. Granato, Physica B **219-220**, 270 (1996).
[39]A. V. Granato, J. Non-Cryst. Solids **307-310**, 376 (2002).
[40]W. Götze and M. R. Mayr, Phys. Rev. E **61**, 587 (2000).
[41]U. Buchenau, N. Nücker, and A. J. Dianoux, Phys. Rev. Lett. **53**, 2316 (1984).
[42]V. K. Malinovsky, V. N. Novikov, P. P. Parshin, A. P. Sokolov, and M. G. Zemlyanov, Europhys. Lett. **11**, 43 (1990).
[43]H. R. Schober and C. Oligschleger, Phys. Rev. B **53**, 11469 (1996).
[44]H. R. Schober, Phys. Rev B **85**, 024204 (2012).
[45]E. J. Saltzman and K. S. Schweizer, Phys. Rev. B **74**, 061501 (2006).
[46]W. Schirmacher, G. Diezemann, and C. Ganter, Phys. Rev. Lett. **81**, 136 (1998).
[47]A. Marruzzo, W. Schirmacher, A. Fratalocchi, and G. Ruocco, Sci. Rep. **3**, 1407 (2013).
[48]A. I. Chumakov, G. Monaco, A. Monaco, W. A. Crichton, A. Bosak, R. Rüffer, A. Meyer, F. Kargl, L. Comez, D. Fioretto, H. Giefers, S. Roitsch, G. Wortmann, M. H. Manghnani, A. Hushur, Q. Williams, J. Balogh, K. Parliński, P. Jochym, and P. Piekarz, Phys. Rev. Lett. **106**, 225501 (2011).
[49]A. Monaco, A. I. Chumakov, G. Monaco, W. A. Crichton, A. Meyer, L. Comez, D. Fioretto, J. Korecki, and R. Rüffer, Phys. Rev. Lett. **97**, 135501 (2006).
[50]K. Niss, B. Begen, B. Frick, J. Ollivier, A. Beraud, A. Sokolov, V. N. Novikov, and C. Alba-Simionesco, Phys. Rev. Lett. **99**, 055502 (2007).
[51]G. Baldi, A. Fontana, G. Monaco, L. Orsingher, S. Rols, F. Rossi, and B. Ruta, Phys. Rev. Lett. **102**, 195502 (2009).
[52]B. Ruta, G. Baldi, V. M. Giordano, L. Orsingher, S. Rols, F. Scarponi, and G. Monaco, J. Chem. Phys. **133**, 041101 (2010).
[53]S. Corezzi, S. Caponi, F. Rossi, and D. Fioretto, J. Phys. Chem. B **117**, 14477 (2013).
[54]X. H. Lin, W. L. Johnson, and W. K. Rhim, Mater Trans. JIM **38**, 473 (1997).
[55]W. H. Wang, P. Wen, D. Q. Zhao, M. X. Pan, T. Okada, and W. Utsumi, Appl. Phys. Lett. **83**, 5202 (2003).
[56]X. H. Lin and W. L. Johnson, J. Appl. Phys. **78**, 6514 (1995).
[57]C. Kittel, *Introduction to Solid State Physics*, 7th ed. (John Wiley & Sons, New York, 1996).
[58]P. W. Anderson, B. I. Halperin, and C. M. Varma, Philos. Mag. **25**, 1 (1972).
[59]C. T. Moynihan, P. B. Macedo, C. J. Montrose, P. K. Gupta, M. A. DeBolt, J. F. Dill, B. E. Dom, P. W. Drake, A. J. Easteal, and P. B. Elterman, Ann. N.Y. Acad. Sci. **279**, 15 (1976).
[60]I. M. Hodge, J. Non-Cryst. Solids **169**, 211 (1994).
[61]A. Q. Tool, J. Am. Ceram. Soc. **29**, 240 (1946).
[62]Z. G. Zhu, P. Wen, D. P. Wang, R. J. Xue, D. Q. Zhao, and W. H. Wang, J. Appl. Phys. **114**, 083512 (2013).
[63]W. H. Wang, J. Appl. Phys. **99**, 093506 (2006).
[64]R. Calemczuk, R. Lagnier, and E. J. Bonjour, J. Non-Cryst. Solids **34**, 149 (1979).
[65]R. Zorn and B. Frick, J. Chem. Phys. **108**, 3327 (1998).
[66]C. Abromeit and H. Wollenberger, Mater. Sci. Forum **15–18**, 523 (1987).
[67]H. v. Löhneysen, H. Rüsing, and W. Sander, Z. Phys. B **60**, 323 (1985).
[68]E. Pérez-Enciso, M. A. Ramos, and S. Vieira, Phys. Rev. B **56**, 32 (1997).
[69]T. Pérez-Castañeda, R. J. Jiménez-Riobóo, and M. A. Ramos, J. Phys.: Condens. Matter **25**, 295402 (2013).
[70]L. Hong, B. Begen, A. Kisliuk, C. Alba-Simionesco, V. N. Novikov, and A. P. Sokolov, Phys. Rev. B **78**, 134201 (2008).
[71]N. Shimodaira, K. Saito, N. Hiramitsu, S. Matsushita, and A. J. Ikushima, Phys. Rev. B **71**, 024209 (2005).
[72]N. Ahmad, K. W. Hutt, and W. A. Phillips, J. Phys. C: Solid State Phys. **19**, 3765 (1986).
[73]V. L. Gurevich, D. A. Parshin, and H. R. Schober, Phys. Rev. B **67**, 094203 (2003).

[This article is copyrighted as indicated in the article. Reuse of AIP content is subject to the terms at: http://scitation.aip.org/termsconditions. Downloaded to ] IP: 159.226.35.24 On: Fri, 18 Apr 2014 01:21:59